Jurnal Teknologi

Full Paper

# FORCE CHARACTERIZATION OF A TUBULAR LINEAR ELECTROMAGNETIC ACTUATOR USING FINITE ELEMENT ANALYSIS METHOD (FEM)

Mariam Md Ghazaly[a*], Tawfik Ahmed Yahya[a], Aliza Che Amran[b], Zulkeflee Abdullah[c], Mohd Amran Md Ali[c], Ahmad Hilkam Jamaludin[a], Nursabillilah Mohd Ali[a]

[a]Center for Robotics and Industrial Automation (CeRIA), Faculty of Electrical Engineering, Universiti Teknikal Malaysia Melaka, Hang Tuah Jaya, 76100 Durian Tunggal, Melaka, Malaysia
[b]Faculty of Technical Engineering, Universiti Teknikal Malaysia Melaka, Hang Tuah Jaya, 76100 Durian Tunggal, Melaka, Malaysia
[c]Faculty of Manufacturing Engineering, Universiti Teknikal Malaysia Melaka, Hang Tuah Jaya, 76100 Durian Tunggal, Melaka, Malaysia

**Article history**
Received
*18 January 2016*
Received in revised form
*17 May 2016*
Accepted
*18 October 2016*

*Corresponding author
mariam@utem.edu.my

## Graphical abstract

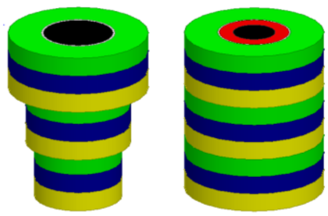

(a)TLRA (b)TLPM

## Abstract

This paper presents an extensive characterising study of two novel electromagnetic actuators, each with different constructions and characteristics aiming to analyse the behaviour and output characteristics of the two designs. The two actuators are Tubular Linear Reluctance Actuator (TLRA) and Tubular Linear Permanent magnet (TLPM) with Halbach array actuator. The study covered the variation of three parameters, which are the actuator air gap, number of turns and actuator size. A comparative section was also presented for the purpose of comparison. The study concentrated extensively on the two characteristics of both actuators known as output thrust force and working range as they are considered as two main concerns of any actuator design. The simulation was used to show the differences between the two designs in many design aspects such as force, displacement and effects of parameters variations. The applied simulation was performed using 3D Finite-element Ansys software, which is capable of showing the magnetic field distribution in the whole actuator and predicting the strength and length of the output stroke.

*Keywords*: Electromagnetic actuator, linear actuator, Halbach array, reluctance , permanent magnet

## Abstrak

Penulisan ini membentangkan kajian dua novel penggerak elektromagnetik dengan penstrukturan dan ciri-ciri yang berbeza dan mengkhususkan kepada analisis terhadap sifat dan ciri-ciri output bagi dua reka bentuk penggerak elektromagnetik. Dua penggerak tersebut adalah penggerak tiub linear berkengganan dan penggerak linear magnet kekal berserta susunan Halbach. Kajian ini merangkumi tiga variasi parameter iaitu jurang udara, bilangan lilitan wayar dan saiz penggerak. Sesi perbezaan juga turut dibentangkan untuk pembandingan. Kajian ini tertumpu kepada teras kuasa dan kemampuan kerja dimana ia adalah dua ciri utama dalam reka bentuk penggerak. Kaedah simulasi digunakan bertujuan memperlihatkan aspek perbezaan dari segi kuasa kerja, kadar anjakan dan kesan daripada parameter yang bervariasi. Simulasi yang digunakan menggunakan perisian *Ansys 3D Finite-element* dimana ia mampu menunjukkan kesuluruhan pengedaran medan magnet bagi dua jenis penggerak dan dapat meramalkan kekuatan dan kepanjangan tujahan.

*Kata kunci*: Penggerak elektromagnetik, penggerak linear, susunan Halbach, daya keengganan, magnet kekal,

# 1.0 INTRODUCTION

Electromagnetic actuators most commonly used in the applications that require high thrust force, high accuracy and various working ranges. The increasing advancements in the usage of the electromagnetic actuators raises the need of improvements especially in terms of output thrust force and working range. Electromagnetic actuators are the most well-known as a linear transmissions work by converting electric and/or magnetic power to linear mechanical motion through magnetic field interactions. Besides that, electromagnetic actuator have lately become an area of interest to a huge number of researchers as they found it has compact sector towards the efficiency and driving improvement, energy saving and significant alternative for many other types of actuators such as piezoelectric and electrostatic actuators. Electromagnetic actuators provide various numbers of advantages over other types of actuators such as higher force and long working range [1]. Because of the advantages that the electromagnetic actuator has, it has led to the increment of the use in many applications such as manufacturing, medical tools, transportation, advance electronic devices, and robotics [2-9].

The electromagnetic actuator consists of two main parts which are the stator (stationary part) and the mover (moving part). Its geometry structure can be classified into two types of main structures which are flat type and tubular type. The tubular type has more rugged mechanical structure as compared to the flat type. The mechanical structure of the tubular type is almost similar with a piston structure [10], [11]. Figure 1 shows the two difference geometry structure type of the linear electromagnetic actuator. The advantages of the tubular type are it can minimised the elimination of stray magnetic field and the force density delivered by the tubular type are is greater than the flat type [12-14].

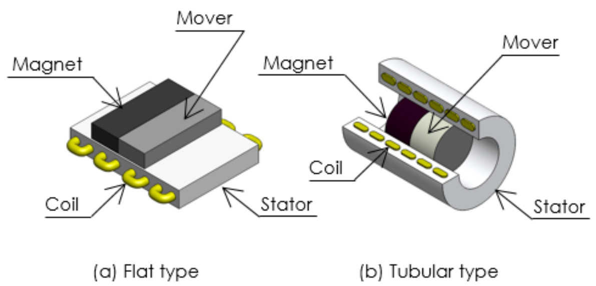


**Figure 1** Two geometry type of electromagnetic actuator

The tubular linear electromagnetic actuator can be categorised into Tubular Linear Permanent Magnet (TLPM) and Tubular Linear Reluctance Actuator (TLRA). The TLPM topologies can be classified into coils and magnet utilisation such moving coil, moving iron and moving magnet [15], [16]. Figure 2 shows the arrangement of the three different topologies of the TLPM. The moving coil type has coils in the mover and permanent magnet (PM) in the stator. The advantage of this type is it has small mover mass and it has high dynamics performance. The disadvantages of this type are it has relatively poor thermal dissipation, low reliability, and bulky size. The moving iron type exhibits high thrust force but its large inertia can cause low dynamic performance resulting less of stability in the actuator. The moving magnet type has a low mass mover but with new design improvements such as Halbach PM array, teeth optimisation and so on, the moving magnet can achieve higher thrust force, higher stability and higher accuracy. Between the three difference configurations of the TLPM actuator topologies, the moving magnet type provide highest efficiency and highest thrust force with excellent servo characteristics [17]. On the other hand, the moving iron type provides some weighted advantages over the other two types in term of simple structure, ruggedness, and the fact that they are relatively inexpensive to be manufactured [18]. Since the TLPM construction's consist of permanent magnet, the cost is high if compare to the TLRA. Instead of the cost of the TLRA is lower, the structure also more simpler as no existance of the permanent magnet [19]. But the disadvantage of the TLRA are it has a high vibration and generate noise sound. In order to obtain the optimum force for both actuators, the actuators must be designed with the optimum design parameter such the air gap thickness [20], [21]. In this paper, both TLRA and TLPM was analyzed using FEM analysis to characterize the force from the varying parameters of actuator designs.

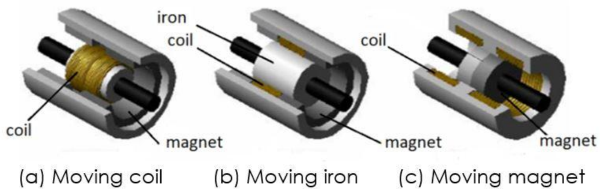


**Figure 2** Three topologies of TLPM actuator

# 2.0 DESIGN STRUCTURE AND INITIAL PARAMETERS

## 2.1 Design 1-Tubular Linear Reluctance Actuator with Step Windings (TLRA)

The Design 1 that is tubular linear reluctance actuator with step windings (TLRA) consists of two main parts which are the stator and the mover. In this design, the stator contains a set of three steps winding coil turns while the mover consists only an iron shaft. Figure 3 shows the geometry structure of Design 1. The dimension details of Design 1 are shown in Figure 4.

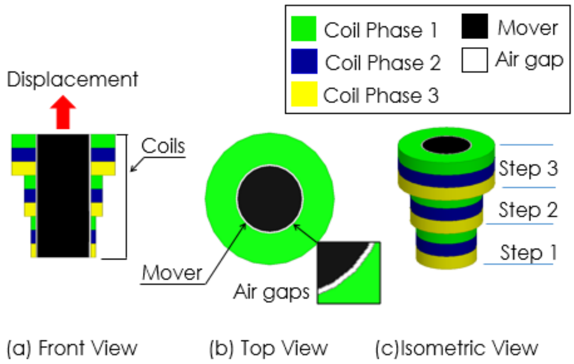


**Figure 3** The Geometric Structure of Design 1-TLRA

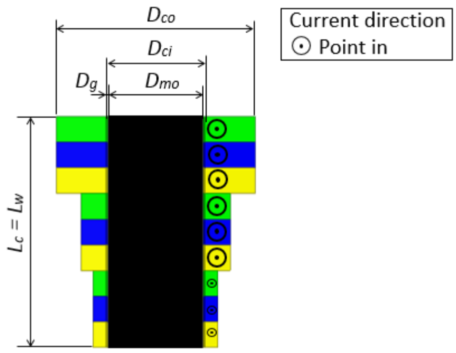


**Figure 4** Current direction and the displacement of Design 1-TLRA

## 2.2 Design 2-Tubular Linear Reluctance Actuator with Halbach Array (TLPM)

The Design 2, namely as the tubular linear permanent magnet (TLPM) with Halbach array actuator consists of two main parts which are the stator and the mover. The stator consists of winding coil turns and the mover consists of iron shaft rounded by permanent magnets inserted in the Halbach array. The Design 2 geometry structures are shown in Figure 5. The directions of current and dimension are illustrated in Figure 6 and Table 2 present the detail dimensions of Design 2.

The differences between the two designs are as follows; in Design 1 structures, the mover consists only an iron shaft and it has the sets of a different number of step windings turns. In Design 2, the mover consists of steel shaft and rounded with permanent magnets that are inserted in the Halbach array and Design 2 has the sets of the same number of step winding turns.

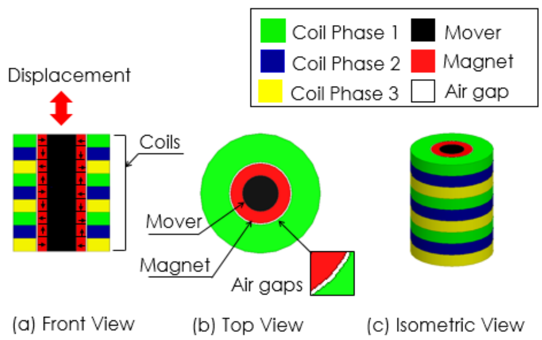


**Figure 5** The Geometric Structure of Design 2-TLPM

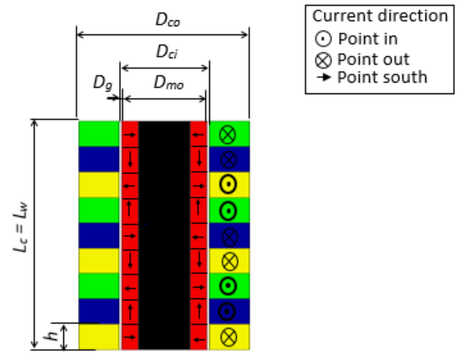


**Figure 6** Current direction and the displacement of Design 2-TLPM

## 2.3 The Initial Parameter of the Design 1 and Design 2

The initial parameters of Design 1 are shown in Table 1 while the initial parameter of the Design 2 are shown in Table 2. In order to compare the optimum force of these two designs, air gap and the number of winding turns are varied.

**Table 1** Initial parameter of Design 1-TLRA

| Parameter | Values | | |
|---|---|---|---|
| Mover outer diameter, $D_{mo}$ | 20mm | | |
| Length of the mover, $L_c$ | 90mm | | |
| Length of the winding, $L_w$ | 90mm | | |
| Conductor diameter, $d_c$ | 0.3mm | | |
| Air gaps (mm), $d_g$ | 0.5mm | | |
| | First Winding | Second Winding | Third Winding |
| Number of turns, $N$ | 17turns | 33turns | 66turns |
| Coil inner diameter, $D_{ci}$ | 21mm | 21mm | 21mm |
| Coil outer diameter, $D_{co}$ | 25mm | 30mm | 40mm |

**Table 2** Initial parameter of Design 2-TLPM

| Parameter | Values |
|---|---|
| Number of turns, $N$ | 66turns |
| Coil inner diameter, $D_{ci}$ | 21mm |
| Coil outer diameter, $D_{co}$ | 40mm |
| Shaft outer diameter, $D_{shaft}$ | 12mm |
| Magnets inner diameter, $D_{mi}$ | 12mm |
| Magnets outer diameter, $D_{mo}$ | 20mm |
| Length of the mover, $L_c$ | 90mm |
| Length of the winding, $L_w$ | 90mm |
| Magnet height, $h$ | 10mm |
| Air gaps (mm), $d_g$ | 0.5mm |

# 3.0 RESULTS

The TLRA with step windings and TLPM with Halbach Array have been designed. All designs specifications have been selected arbitrarily under two conditions; the designs should be small and the maximum stroke is 90 mm. In this section, the result obtained presents the magnetic field distribution and the effects of the force when parameters of air gap, winding turns and actuator's size scales are varied.

## 3.1 Magnetic Field Distribution

### *3.1.1 Magnetic Field Distribution of Design 1 (TLRA)*

The magnetic field distribution in the Design 1 actuator is shown in Figure 7(a). The strongest field is produced at the centre of the actuator, followed by the top, then the minimum magnetic field distribution is produced at the bottom of the actuator where the minimum number of turns are implemented. The strength of the magnetic field in the displacement region identifies the strength of the force produced. Figure 7(b) shows the top view of the TLRA's magnetic field distribution, the maximum magnetic field is produced around the mover's edges and it getting lesser towards the centre of the mover.

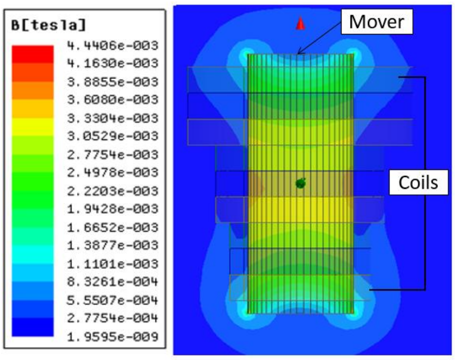


(a) Design 1 TLRA Magnetic Distribution-Front View

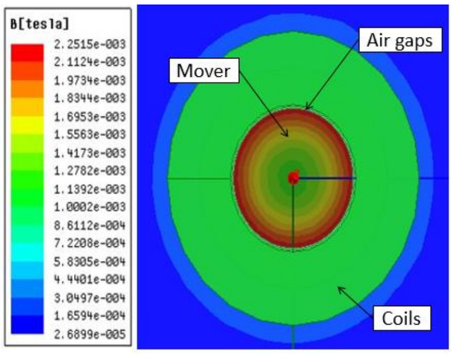


(b) Design 1 TLRA Magnetic Distribution-Top View

**Figure7** Magnetic field distribution of Design 1 (TLRA)

### *3.1.2 Magnetic Field Distribution of Design 2 (TLPM)*

The magnetic field distribution depends on how the magnetic field produced from the coils that are aligned with the magnetic field produced by the magnets. Figure 8(a) shows the strongest magnetic field is produced in magnet numbers 1, 3, 5, 7 and 9, where the magnetisation direction of the magnets is in the x-direction aligned with the magnetic field produced by the coils. The magnetic field produced in the air gap region causing the force on the mover is divided into four regions, each with a height of 2h where h is the height of one magnet. This distribution indicates that the stroke will be short and be repeated every 2h, which is 20 mm in this design. In addition, Figure 8(b) shows the top view of the magnetic field distribution in the actuator where the magnetisation direction of the magnet is in the x-direction. The maximum of the magnetic field occurred at the edges of the mover where the magnetic field of the magnet and the coil are aligned together. On the other hand, the magnetic field in the z-direction is equally distributed around the mover diameter. It is because of the magnetic field of the coils does not aligned with the magnetisation direction of the magnet as shown in Figure 8(c).

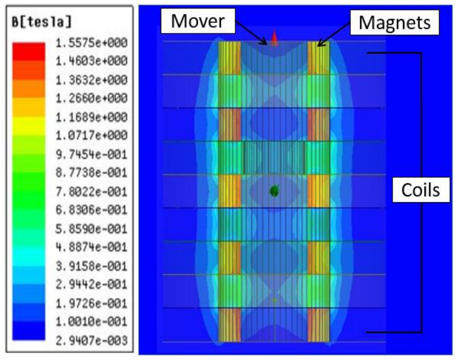


(a) Design 2 TLPM Magnetic Distribution-Front View

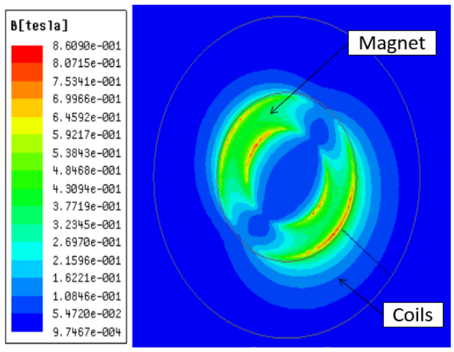


(b) Design 2 TLPM Magnetic Distribution at x-direction-Top View

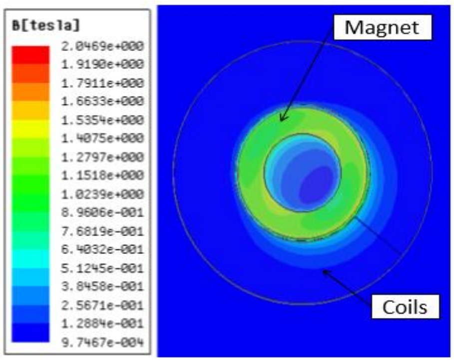


(c) Design 2 TLPM Magnetic Distribution at z-direction-Top View

**Figure 8** Magnetic field distribution of Design 2 (TLPM)

## 3.2 Thrust Analysis

### *3.2.1 Thrust Analysis of Design 1 (TLRA) in Positive Direction*

In this section, the thrust force for TLRA with the step windings is analysed in both positive and negative directions. The displacement of the mover is shown in Figure 9. It is obviously noticed as the mover get closer to the centre position of the coil, the force is increased due to the change of the reluctance inside the actuator. At the end of the stroke which is 90 mm, a near-to-zero force is applied on the mover. The highest force generated in the actuator is at 5-30 mm of the displacement, where the difference in inductance is at its maximum. The lowest force is at 90 mm of the displacement where the difference in inductance is almost zero. The longest stroke with considerable of the force obtained by this actuator is 70 mm, which proves that the function of the steps winding is to get the maximum stroke with the highest possible of force.

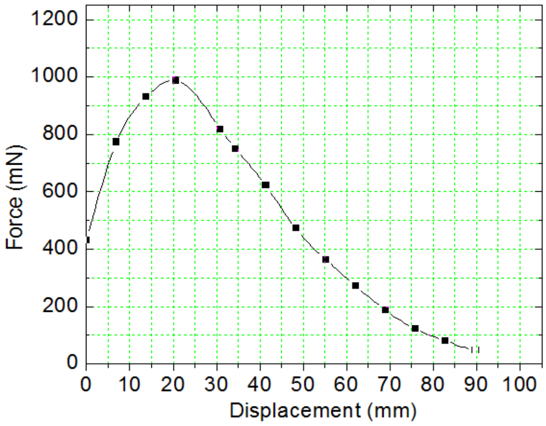


**Figure 9** Displacement in positive direction-Design 1 (TLRA)

### 3.2.2 Thrust Analysis of Design 1 (TLRA) in Negative Direction

When reversing the direction of displacement to the negative direction, the mover does not move at all. It is because there is no enough force to move it and the reluctance is maximum at the centre. This proves the theory stated in the literature review section, which claims that the actuator only pulls but never pushes. Figure 10 shows the force VS the displacement in the negative direction have no displacement occurs.

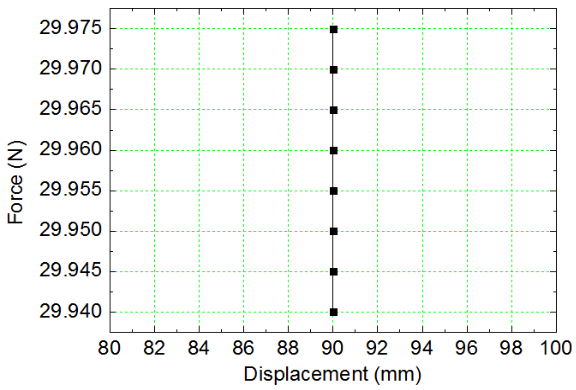


**Figure 10** Displacement in negative direction-Design 1 (TLRA)

### 3.2.3 Thrust Analysis of Design 2 (TLPM) in Positive Direction

As seen in Figure 11, the thrust force produced in this design is a sinusoidal-like waveform. The actuator performs a complete cycle of a sinusoidal waveform at 20 mm, which is equivalent to the height of two magnets ("h" is the height of the magnet). This situation keeps repeating the same sinusoidal waveform with the thrust force is decreases as the mover is displaced far from the centre of the actuator. For the positive direction, the peak force is produced at 0.5 h (5 mm), followed with 1.5 h (30 mm), 2.5 h (50 mm), 3.5 h (70 mm) and 4.5 h (90 mm). In contrast, for the negative direction, the peak force is produced at -0.25 h (-5 mm), -1.5 h (-30 mm), -2.5 h (-50 mm), 3.5 h (70 mm) and 4.5 h (90 mm). The design exhibits controllable high force servo characteristics needed by a vast variety of applications where precision, high force and short stroke are required.

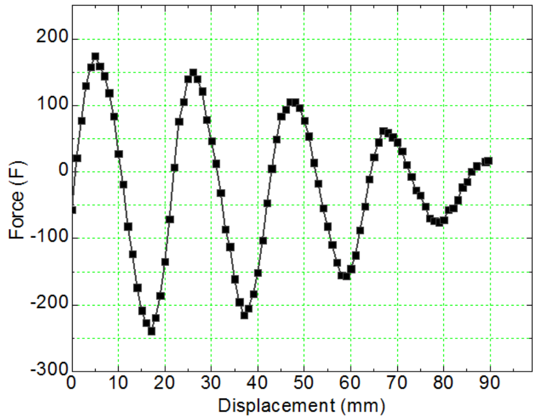


**Figure 11** Displacement in positive direction-Design 2 (TLPM)

### 3.2.4 Thrust Analysis of Design 2 (TLPM) in Negative Direction

Figure 12 shows the displacement of the mover when the stroke direction is changed to the negative direction, the mover displacement start from -90 mm. The force characteristics are same as the positive direction. The force wave is increase as the mover is displaced to the centre of the actuator.

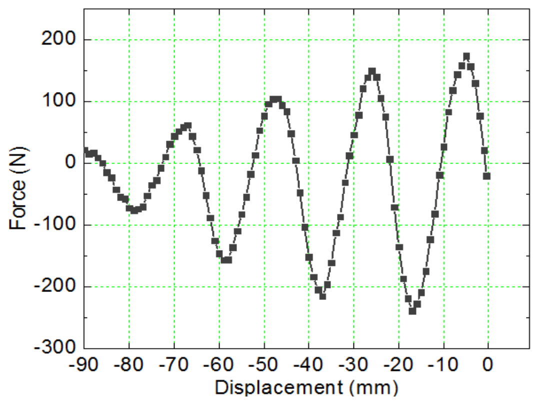


**Figure 12** Displacement in negative direction-Design 2 (TLPM)

## 3.3 Parameters Variations

### 3.3.1 Air Gap Variation for Design 1 (TLRA)

The air gap is varied from 0.5 mm to 1.5 mm with 0.2 intervals. In this analysis, the input current is increased from 0 A to 20 A. Figure 13 shows the results of the force produced when the air gaps are varied. The thrust force reaches 55 N in when 0.5 mm air gap is used while it reaches only 45 N in when 1.5 mm is used. This is due to the magnetic field gets weaker as the distance between the coil and the steel mover gets larger. The force that is produced from 0.5 mm, 0.7 mm and 0.9 mm air gaps are higher than the other air gap sizes. We can conclude from the variations of the air gaps that the force decreases as the air gap between the stator and mover gets larger. However, the air gap cannot be less than 1 mm due to the mechanical limitations.

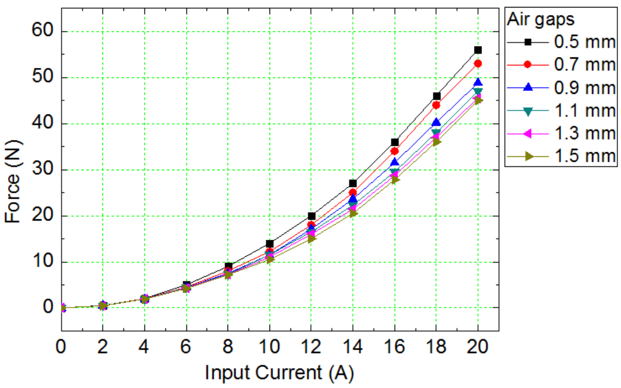


**Figure 13** Effects of varying air gap thickness-Design 1 (TLRA)

### 3.3.2 Air Gap Variation for Design 2 (TLPM)

In this design, the air gap is varied two times; one time for the small gap from 0.5 mm to 1.5 mm, and the other time compares the original 0.5 mm with two high values 2 and 2.5 mm. The result of the force for six different small air gap sizes between the tubular linear permanent magnet and Halbach array actuator are shown in Figure 14. The graph shows the force in response to the applied current from 0 to 20 A. In addition, the variant of air gap's parameter produced linear behaviour of the force corresponded to the input current. Moreover, the starting force for each air gap variant is different and caused by the magnetic field generating consequence to the air gap size. For the smallest air gap, which the dimension of the air gap is 0.5 mm, the starting force is -0.1 N and reaches 24 N when the 20 A current is applied. For the largest air gap dimension of 1.5 mm, the starting force is 62 N and reaches 85 N when 20 A is applied.

Figure 15 shows the force VS input current for three different sizes of air gaps. The initial air gap dimension is 0.5 mm and two large sizes of air gaps: 2 mm and 2.5 mm. For instance, the produced force starts to greatly decrease when the air gaps are 2 mm and more. The force produced with 0.5 mm is 24 N but only around 6 N when the gap is more than 2 mm that the starting force also starts to decrease. This behaviour is caused by the magnetisation effect due to the air gap size becoming too large.

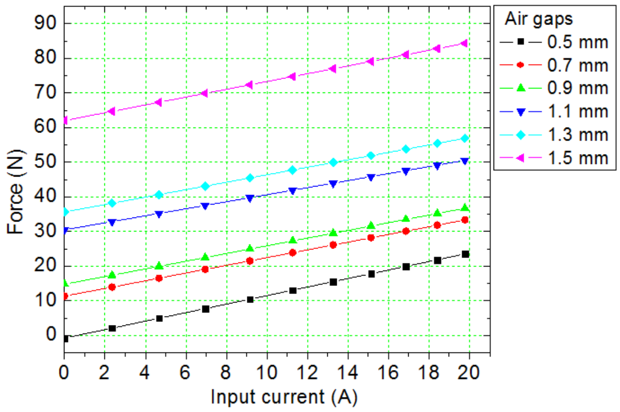


**Figure 14** Effects of varying air gap thickness-Design 2 (TLPM)

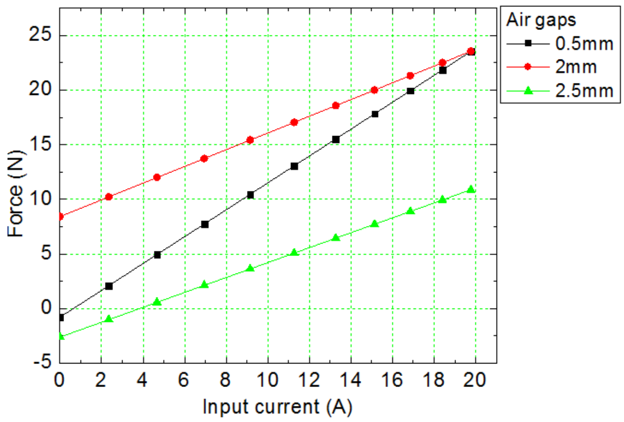


**Figure 15** Effects of varying large size air gaps thickness-Design 2 (TLPM)

### 3.3.3 Varying Number of Turns Design 1 - TLRA

The set of the three-step winding number of turns is varied for five sets. The parameter of step winding sets is shown in Table 3.

**Table 3** Sets of number of turns for the three steps windings of Design1 (TLRA)

| Steps | Number of turns | | | | |
|---|---|---|---|---|---|
| | Set 1 | Set 2 | Set 3 | Set 4 | Set 5 |
| Step 1 | 25 | 50 | 75 | 100 | 125 |
| Step 2 | 50 | 100 | 150 | 200 | 250 |
| Step 3 | 100 | 200 | 300 | 400 | 500 |

From Figure 16, the force increases as the number of turns at each step windings increase. The applied current varies from 0 to 20 A. At the maximum input current 20 A, set 1 produces the smallest force (75 N) and set 5 produces the greatest force (760 N). For the first three sets of step winding's number of turns, the force increment is small, between 50 to 100 N but when a large number of turns is applied for sets 4 and 5, the force increment from steps 3 and 4 is large (175 N) and the increment between both sets is 325 N.

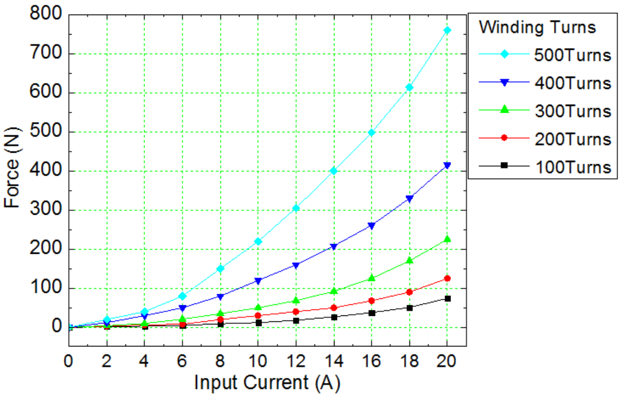


**Figure 16** Effects of varying number of winding turns-Design 1 (TLRA)

### 3.3.4 Varying Number of Turns Design 2 (TLPM)

The number of winding turns are varied in order to see the behaviour of the force corresponding to each of the variation. Five sets of a different number of turns with an interval of 100 turns are set up as shown in Table 4.

**Table 4** The variant of number of turns for Design 2 (TLPM)

| Number of turns | | | | |
|---|---|---|---|---|
| Set1 | Set2 | Set3 | Set4 | Set5 |
| 100 | 200 | 300 | 400 | 500 |

The generated force increases as the number of turns increase as shown in Figure 17. The force produced by 100 turns is 43 N and starts to increase regularly as the number of turns increases until it reaches 134 N for 500 turns. Besides that, the starting force caused by magnets is as same as the size of the magnets that is not changed.

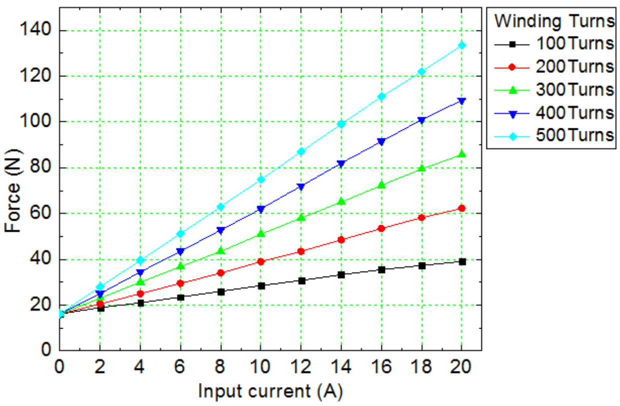


**Figure 17** Effects of varying numbers of winding turns-Design 2 (TLPM

### 3.3.5 Varying Sizes of Design 1 (TLRA)

Six different sizes of actuators are varied and analysed. The scales varied are the original size, 20%, 40%, 60%, 80% and 100% larger. The graph in Figure 18 shows the induced force acting on the plunger for the six different sizes VS different values for the input current, ranging from zero to 20 A. The graph also shows that the forces for original and 20 % larger are almost the same and the small change between 40% and 60%, also the smaller change between 80% and 100%. We can suggest that as the size increases, the force also induces. Besides that, the original sizes for 40% and 80% are far better choices that can save cost and produce high forces. This is due to the small difference between the output force of 40% and 60% of the actuator's size scale variants. The same goes for 80% and 100% of the actuator's size variants.

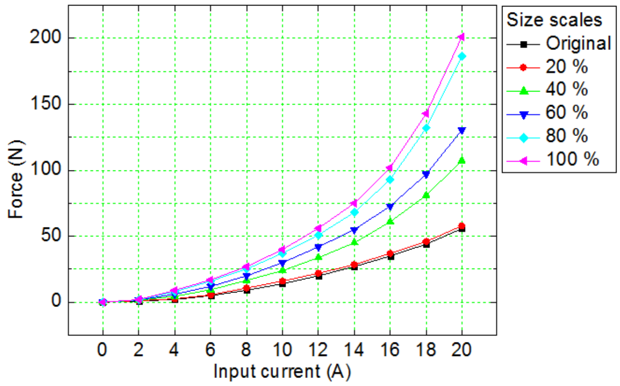


**Figure 18** Effects of varying size scales – Design 1 (TLRA)

### 3.3.6 Varying Sizes of Design 2 (TLPM)

The force of different sizes of Tubular Linear Permanent Magnet with Halbach Array Actuator are analysed and the result of actuator's generated forces are obtained. This is proven starting from the original size and increasing the size by 20% at a time until the size is doubled at 100% increment.

The results of produced force VS input current for six different sizes of the actuator are presented in Figure 19. The results indicate great difference in resulting force as the size are varies. Also, the force increases as the size increases. The best size would be 100 % larger than the original as it shows a large output force difference than the 80% of the size scale.

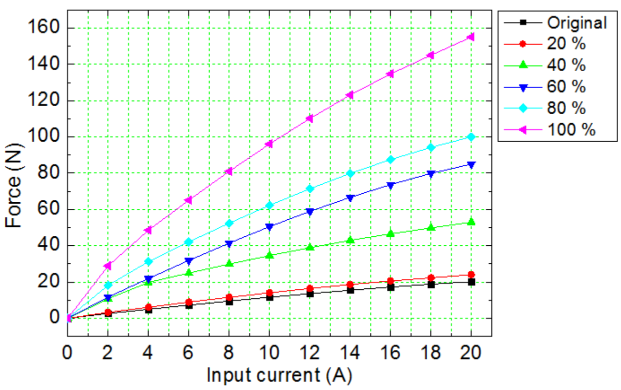


**Figure 19** Effects of varying size scales - Design 2 (TLPM)

### 3.4 Characteristic Comparison between Two Designs

The comparison of thrust between two designs are shown in Table 5. Design 1 (TLRA) has better stroke compare to Design 2 (TLPM). Design 2 (TLPM) has advantages of a larger force, dual displacement direction and smaller starting force. The characteristic comparison between the initial parameter for both designs are presented in Table 5.

**Table 5** Characteristics comparison between the initial parameter of the two designs

| Characteristic | Design 1 (TLRA) | Design 2 (TLPM) |
|---|---|---|
| Maximum Force (N) | 1 | 185 |
| Stroke (mm) | 70 | 20 |
| Displacement Direction | Positive | Positive and negative |
| Starting Force (N) | 0.4 | -50 |

The effect of varying parameters correspond to the force are shown in Table 6. When varying the actuator air gap thickness between the stator and the mover of the actuator, the force produced decreases as the size of the air gap increases. Larger number of winding turns produces larger force and bigger size scale of the actuator produce larger force. The optimum parameter of both Design 1 and Design 2 are presented in Table 7.

**Table 6** Comparison of parameters variations between the two designs

| Parameter | Design 1 (TLRA) | Design 2 (TLPM) |
|---|---|---|
| Air gap | The produced force decreases as the size of air gap increases | *Smaller air gap:* Only the starting force decreases. *Larger air gap (2mm and higher):* The produced force decreases as the size of air gap increases |
| Number of turns | The higher number of turns will generate more force | The higher number of turns will generate more force. |
| Size scale | The larger scale's size will generate more force. | The larger scale's size will generate more force. |

**Table 7** The optimum parameter for Design 1 and Design 2

| Varying Parameter | Design 1 (TLRA) | Force (TLRA) | Design 2 (TLPM) | Force (TLPM) |
|---|---|---|---|---|
| Air gap thickness | 0.5mm | 55N | 1.5mm | 85N |
| Number of winding turns | Set5 : Step1: 125turns Step2:250 turns Step3:500 turns | 760N | 500turns | 134N |
| Size scales | 100% | 205N | 100% | 155N |

## 4.0 CONCLUSION

The tubular linear reluctance actuator with step windings and tubular linear permanent magnet with Halbach array actuator were designed and 3D FEM Ansys Maxwell were used to clarify the validity of the designs. The magnetic field distribution, the thrust force, the displacement, and the effects of the varying parameters of air gap size, number of turns and size scale were analysed in order to characterize the force characteristics of the two designs. The step winding structure for the reluctance actuator has been proven to significantly improve the reluctance actuator performance and generate more force and longer stroke. Nevertheless, this design still suffers from two disadvantages; high current needed in order to generate high force and it also has high vibration. Besides that, the permanent magnet actuator exhibited high force due to the use of magnet that are arranged with the Halbach array arrangement but it still produce short stroke. The Maxwell FEM analysis proves that the permanent magnet actuator produced more force than reluctance actuator but with much smaller stroke. Hence, permanent magnet actuator is preferred in applications where high force, low voltage and short stroke are required. The reluctance actuator is preferred where high voltage is available and long stroke is required. More studies for both designs are recommended to overcome the low force for reluctance actuator and short stroke for permanent magnet actuator. From the result obtained, it can be concluded that the TLRA produced optimum force which are 760N with the parameter of 0.5 mm air gaps and 300 of winding turns.

## Acknowledgement

Authors are grateful to Universiti Teknikal Malaysia Melaka (UTeM) for supporting the research. This research and its publication are supported by Research Acculturation Collaboration Effort (RACE) grant, no.RACE/F3/TK5/FKE/F00249 and Center for Research and Innovation Management (CRIM).

## References


[1] M. M. Ghazaly, L. T. Kang, C. Y. Piaw, and S. Kaiji. 2015. Force Optimization of an Force Artificial Muscle Actuated Underwater Probe System using Linear Motion Electrostatic Motor. *J. Teknologi*. 9(2): 113-118.

[2] W. R. Cawthorne and S. Petreanu.1999. Development of A Linear Alternator-engine for Hybrid Electric Vehicle Applications. *IEEE Trans.* 48(6): 1797-1802.

[3] W. J. Kim, D. L. Tumper and J. H., Lang. 1998. Modelling and Vector Control of Planar Magnetic Levitator. *IEEE Trans. On Industry Applications*. 34(6): 1254-1262.

[4] J. Lin, K. W. E. Cheng, Z. Zhang, N. C. Cheung and X. Xue. 2015. Adaptive Sliding Mode Technique-based Electromagnetic Suspension System with Linear Switched Reluctance Actuator. *IET Electric Power Applications*. 9(1): 50-59.

[5] J. Ji, Z. Ling, J. Wang, W. Zhao, G. Liu and T. Zheng. 2015. AU-30 Design and Analysis of a New Halbach Magnetized Magnetic Screw for Artificial Hearts. *IEEE Trans. Magn*. 47(10): 4480.

[6] K. H., I. B. and K. Krasteva. 2011. Static Force Characteristics of Electromagnetic Actuators for Braille Screen. *ELEC. ENERG*. 24(2): 157-167.

[7] J. Ponmozhi, C. Frias, T. Marques, and O. Frazo. 2012. Smart Sensors/Actuators For Biomedical Applications: Review. Meas. *J. Int. Meas. Confed.* 45(7): 1675-1688.

[8] K. M. Lee, Y. Kim, J. K. Paik, and B. Shin. 2015. *Clawed Miniature Inchworm Robot Driven by Electromagnetic Oscillatory Actuator.* 2015. *J. Bionic Eng*. 12(4): 591-526.

[9] J. Zhu, H. L and Y. Guo. 2005. A Tubular Linear Motor for Micro Robotic applications. *IEEE Int. Conf. Mechatronics*. Taipei, Taiwan. 596-601.

[10] B. M. Dutoit, P. A. Besse, and R. S. Popovic. 2003. Planar Multidipolar Electromagnetic Actuators. *IEEE Trans. Magn*. 39(2): 1026-1034.

[11] B. Lesquesne. 1996. Permanent Magnet Linear Motors for Short Strokes. *IEEE Trans. On Industry Applications*. 32(1): 161-168.

[12] J. Wang, D. Howe and G. W. Jewell. 2004. Analysis and Design Optimization of an improved Axially Magnetized Tubular Permanent Magnet Machine. *IEEE Trans. Energy Convers*. 19(2): 289-295.

[13] Z. Q. Zhu, P. J. Hor, D. Howe and J. R. Jones. 1997. Novel Linear Tubular Brushless Permanent Magnet Motor. *Int. Conf. Electr. Machines Drives*. Cambridge, MA. 444: 91-95.

[14] K. Halbach. 1981. Design of Permanent Multipole Magnet with Oriented Rate Earth Cobalt Material. *Nuclear Instruments and Method*. 169(1): 1-10.

[15] J. F. Eastham, R. Akmese and H. C. Lai. 1990. Optimum Design of Brushless Tubular Linear Machines. *IEEE Trans. On Magnetics.* 26(5): 2547-2549.

[16] C. Urban and R. Witt. 2012. Development of a Bendable Permanent-Magnet Tubular Linear Motor. *IEEE Trans on Magnetic.* 48(8): 2367-2373.

[17] N. Bianchi, S. Bolognani and F. Tonel. 2001. Design Consideration for a Tubular Linear PM Servo Motor. *EPE J.* 11(3): 41-47.

[18] Z. Q. Zhu and D. Howe. 2001. Halbach Permanent Magnet Machines and Applications : A REVIEW. *IEE Proc.-Electr. Power Appl.* 148(4): 299-308.

[19] J. F. Pan, Y. Zou, and G. Cao. 2013. An Asymmetric Linear Switched Reluctance Motor. *IEEE Trans. Energy Convers*. 28(2): 444-451.

[20] J. Lee, E. M. Dede, D. Banerjee, and H. Iizuka. 2012. Magnetic Force Enhancement in A Linear Actuator by Air-gap Magnetic field Distribution Optimization and Design. *Finite Elem. Anal. Des.* 58: 44-52.

[21] Y. Li, T. Cheng, D. Xuan and Y. Shen. 2015. Force Characteristic of a Mnetic Actuator for Separable Electric Connector based on Conical Air gap. *Advance in Mechanical Engineering.* 7(2): 1-8.